communications biology

A Nature Portfolio journal

Article

https://doi.org/10.1038/s42003-025-08298-z

High-fat diet induces pre-eclampsia through dampening cell-autonomous C3 in trophoblasts

Simeng Zhu[1,2,3,8], Siyue Chen[2,8], Yingzhou Ge[2], Fangyue Zhou[2], Kaizhen Su[4], Congfeng Xu[1] ✉, Yanting Wu[2,5,6] ✉ & Hefeng Huang[2,3,4,5,6,7] ✉

Hyperlipidemia contributes to low-grade inflammation and abnormal immune response, which is putatively involved in the development of pre-eclampsia (PE). As components of innate immune system, complements play a critical role in regulating inflammation. However, how cell-autonomous complement changes and works in PE remains elusive. In the current study, we established L-NAME-induced mice to manifest PE-like symptoms. In presence of high-fat diet (HFD) feeding, the PE-like symptoms were considerably aggravated, as well as down-regulated complement C3 in HFD/L-NAME mice trophoblasts. To explore the effect of C3 in PE development, we generated C3 overexpression and knockdown cell (Swan.71^{C3} and Swan.71$^{\Delta C3}$) based on Swan.71, a trophoblast cell line. We found that Swan.71^{C3} cells display promoted proliferation, migration and invasion capability and less secretion of anti-angiogenetic cytokines, while Swan.71$^{\Delta C3}$ showed highly-activated NLRP3 inflammasome and pyroptosis, which was also noted in HFD/L-NAME placentas, highlighting the contributing role of inflammation to PE. Indeed, pro-inflammatory cytokines were increased in placentas from HFD/L-NAME mice. The similar trends of C3 in trophoblast from severe PE patients supported the contribution role of C3 to PE pathogenesis. Thus, our study provides evidence that cell-autonomous complement C3 regulates NLRP3 inflammasome activation upon HFD exposure, affecting trophoblast cell function in PE development.

Manifested as new-onset of gestational hypertension after 20 weeks of pregnancy and multi-organ dysfunction, such as cardiovascular, hepator-enal, and coagulation systems[1], pre-eclampsia (PE) affects about 2–4% of pregnant women worldwide, and is usually associated with higher maternal and fetal morbidity and mortality[2]. So far, there is no effective treatment for PE except placenta expulsion, and more efforts are urgent to investigate the pathological mechanism of PE development. During early pregnancy, extravillous trophoblast (EVT) invade from placental villus into the decidua and myometrium to replace spiral artery endothelial cells and destroy peri-vascular smooth muscle cells, known as spiral artery remodeling[3]. Spiral artery remodeling lowers vessels resistance to meet the increased demand of maternal-fetal nutrients and gas exchange. Poor placentation in this stage (first pregnancy trimester) is widely believed as the major cause of PE, which is due to inadequate EVT invasion and artery remodeling, and results in placental ischemia and induces inflammation and oxidative stress, aggra-vating trophoblast dysfunction. Reciprocally, the stressed trophoblasts secrete inflammatory cytokines and anti-angiogenetic factors, including sFlt-1 (soluble FMS-like tyrosine kinase-1) and sEng (soluble Endoglin), leading to more severe systematic maternal endothelial dysfunction[4].

It has been shown that obese pregnant women are more likely to develop maternal and fetal comorbidities, including gestational diabetes, macrosomia, and hypertension disorders. Pregnant women with obesity usually show a disturbed lipidemia profile, such as hyperlipidemia. Both hyperlipidemia and obesity have been identified as major risk factors for PE[5,6]. The elevated cholesterol promotes atherosclerosis and induces pla-cental endothelial cell dysfunction, activates inflammatory pathways, and

[1]Department of Cardiology, Sixth People's Hospital, Shanghai Jiaotong University School of Medicine, Shanghai, China. [2]Obstetrics and Gynecology Hospital, Institute of Reproduction and Development, Fudan University, Shanghai, China. [3]International Peace Maternity and Child Health Hospital, Shanghai Jiao Tong University School of Medicine, Shanghai, China. [4]Key Laboratory of Reproductive Genetics (Ministry of Education), Department of Reproductive Endocrinology, Women's Hospital, Zhejiang University School of Medicine, Hangzhou, China. [5]Research Units of Embryo Original Diseases, Chinese Academy of Medical Sciences, Shanghai, China. [6]Shanghai Key Laboratory of Reproduction and Development, Shanghai, China. [7]State Key Laboratory of Cardiology, Shanghai, China. [8]These authors contributed equally: Simeng Zhu, Siyue Chen. ✉e-mail: cxu@shsmu.edu.cn; yanting_wu@163.com; huanghefg@hotmail.com

stimulates sFlt-1 secretion, thus inducing placental ischemia[7]. Besides, obesity drives abnormal immune response, such as chronic inflammation. Elevated expression of TLR4 (Toll-like receptor 4), MCP-1 (Monocyte chemoattractant protein 1), and IL(Interleukin)-1β has been found in the placenta of an obese monkey. Additionally, obesity triggers the activation of NLRP3 (NOD-, LRR-, and pyrin domain-containing protein 3) inflammasome[8], leading to placental inflammation. Taken together, these suggest that the immune system could play a crucial role in poor placentation and PE development[9].

The complement system is one of the most ancient parts of the immune system, and is involved in inflammation and clearance of microbes and injured cells. Previous studies suggested variants of maternal and fetal complement genes, like *C3*, *CFH* (complement factor H), and *CD46*, were highly prevalent in PE patients[10,11], proposing their potential role in the pathogenesis of PE. Meanwhile, hyperlipidemia and obesity were positively associated with elevated complement component levels[12,13]. Recent studies have shown that there are intracellular complements in multiple cell types, and play critical functions in various cellular processes. For example, in T helper 1 cells, activated C5 initiates the generation of ROS (reactive oxygen species) and promotes inflammasome assembly[14], and intracellular C3 mediates mTOR (mammalian target of rapamycin) pathway activation and maintains $CD4^+$ T cell homeostasis[15]. Cell-autonomous complement components were also found in epithelial cells, endothelial cells, fibroblasts, and pancreatic β cells, promoting autophagy and tumorigenesis[16,17]. However, the role of complement components in trophoblasts has not been elucidated. In this study, we aimed to examine the cell-autonomous complement levels in trophoblasts from PE patients and the high-fat diet (HFD) mice model, and the effect of C3 on the function of trophoblasts to elucidate the role of cell-autonomous complements during PE development.

Results

HFD aggravated PE-like symptoms in mice

HFD-induced hyperlipidemia has been shown to contribute to multiple disorders, such as metabolic, cardiovascular disorders, and PE. To verify the effect of lipids in PE development, we constructed PE-like mice model with L-NAME (L-arginine methyl ester) combined with or without HFD. After 8 weeks of HFD feeding, L-NAME/HFD mice displayed evident hyperlipidemia (Supplementary Table 1), and higher SBP (systolic blood pressure), compared with that in L-NAME group at E9.5 (Fig. 1a), showing a clear positive relevance. And 24 h-urine albumin/creatine ratio was also elevated in HFD/L-NAME mice compared with that in NCD (normal chew diet)/L-NAME group (Fig. 1b). While there was no difference in the placenta weight (Fig. 1c), the fetus from HFD/ L-NAME mice displayed smaller size and decreased body weight than those in NCD/L-NAME group (Fig. 1d, e) at E18.5. In this study, fetal weight less than the 10th percentile of control mice without L-NAME digestion was defined as fetal growth restriction (FGR). Increased FGR rate was also observed in HFD/L-NAME group compared to NCD/L-NAME mice (Fig. 1f). These results collectively suggest that HFD aggravates PE-like symptoms in mice.

HFD decreased complement C3 level in mice placentas

In order to explore the mechanism underlying the effect of HFD on PE, we detected the mice placental inflammatory cytokines, and IL-1β, IL-6, and IL-18 were significantly increased in HFD fed placentas (Fig. 2a). Cell-autonomous complement system is a potential driver of inflammation, thus its main component, C3 and C5 were subsequently detected. C3 was significantly down-regulated in HFD-fed placentas, especially in HFD/L-NAME placentas (Fig. 2b, confirmed with a standard control in Supplementary Fig 1a). Further, IHC (Immunohistochemistry) staining showed that C3 complement was reduced in HFD/L-NAME treated trophoblasts compared with L-NAME (Fig. 2c). However, there was no significant variation for complement component C5 based on IHC staining between HFD and NCD groups (Supplementary Fig 1b), suggesting the potential functional role of C3 for hyperlipidemia-aggravated PE, putatively by affecting the function of trophoblast.

Decreased C3 expression in severe PE placentas

To verify that complements are clinically involved in the pathogenesis of PE, we collected placenta tissue samples from four normal pregnant women, four mild and four severe PE patients, respectively. The clinical characteristics of enrolled patients are listed in Table 1. While the lipid levels were higher in severe PE patients and mild PE patients compared with normal pregnant women, we found no significant differences between them. The expression of complements was evaluated by immunoblotting assay, and the results indicated that C3 expression was significantly downregulated in placental tissues from severe PE patients, compared with normal placentas and mild PE placentas, while there was no considerable change on C5 between PE and control placentas (Fig. 3a). The C3 and C5 were confirmed by standard C3 protein (MyBioSource, #MBS2888861), C3b protein (Cell Sciences, #CSI19503), iC3b (Cell Sciences, #CSI19503, Supplementary Fig 2a) and C5 protein (MyBioSource, #MBS147387) (Supplementary Fig 2b). So we focused our research on C3 in the following studies. To further investigate the distribution of C3, IHC staining was performed with placenta sections, and we found that C3 was mainly expressed in trophoblasts (Fig. 3b). Compared with normal placentas and mild PE placentas, C3 expression was decreased in severe PE placentas (Fig. 3b), supporting the assumption that C3 expression is functionally involved in the PE pathogenesis. The colocation of C3 and trophoblasts was further confirmed with confocal microscopy (Supplementary Fig 2c). Additionally, severe PE placentas had higher IL-1β, IL-6, and IL-18 levels (Table 1), which are consistent with those of the animals, mirroring the reliability and propriety of the animal model to explore how complement works in HFD/L-NAME-induced PE.

Effects of C3 on trophoblast cellular behaviors

In order to investigate the role of C3 for trophoblast function, we established stable Swan.71 cell line with C3 overexpression (Swan.71^{C3}) and C3 knockdown by successive selection (Swan.$71^{\Delta C3}$), confirmed by C3, C3b, iC3b standard controls (Fig. 4a). Taking these cell lines, we have detected the common cellular behaviors, such as proliferation, migration, and invasion, which are critical features of trophoblasts for pathogenesis of PE[18]. As shown in Fig. 4b, Swan.71^{C3} cells possess notably increased cell proliferation capabilities. We employed wound healing assay and transwell assay to detect cellular migration and invasion capabilities of trophoblasts, and our results demonstrated that Swan.71^{C3} had promoted migration and invasion effect, while the cellular motility and invasion were largely suppressed in Swan.$71^{\Delta C3}$ cells (Fig. 4c, d). Besides, Swan.71^{C3} cells showed a decreased rate of apoptosis compared with the empty vector group, while more apoptosis was observed in Swan.$71^{\Delta C3}$ cell (Fig. 4e). The gating strategy of flow cytometry was shown in Supplementary Fig 3. These data show that C3 has multiple effects on trophoblast behaviors, such as proliferation, migration, invasion, and apoptosis, which are fundamental for PE progression. More importantly, knockdown of C3 increased anti-angiogenetic cytokines sFlt-1 and sEng, which are soluble antagonists of VEGF (vascular endothelial growth factor) and TGF-β (transforming growth factor-β), while VEGF secretion was inhibited (Supplementary Fig 4). Collectively, these results demonstrate the essential role of cell-autonomous C3 for trophoblast cell function, thus consequently for PE pathogenesis.

Cell-autonomous C3 regulated inflammatory cytokines secretion

As a key effector and regulator for innate immunity, cell-autonomous C3 has been shown to be critical for inflammation processes and inflammatory diseases[19–21]. Given the essential role of inflammation during the pathogenesis of PE, it is reasonable to further explore whether cell-autonomous C3 expression induces inflammation in trophoblasts. So we then collected supernatant from cultured Swan.71 cells and detected the production of cytokines such as IL-6, TNF-α (Tumor Necrosis Factor-α), and IFN-γ (Interferon-γ), which have been shown to contribute to PE development[22]. Based on the ELISA assay, our results showed that the

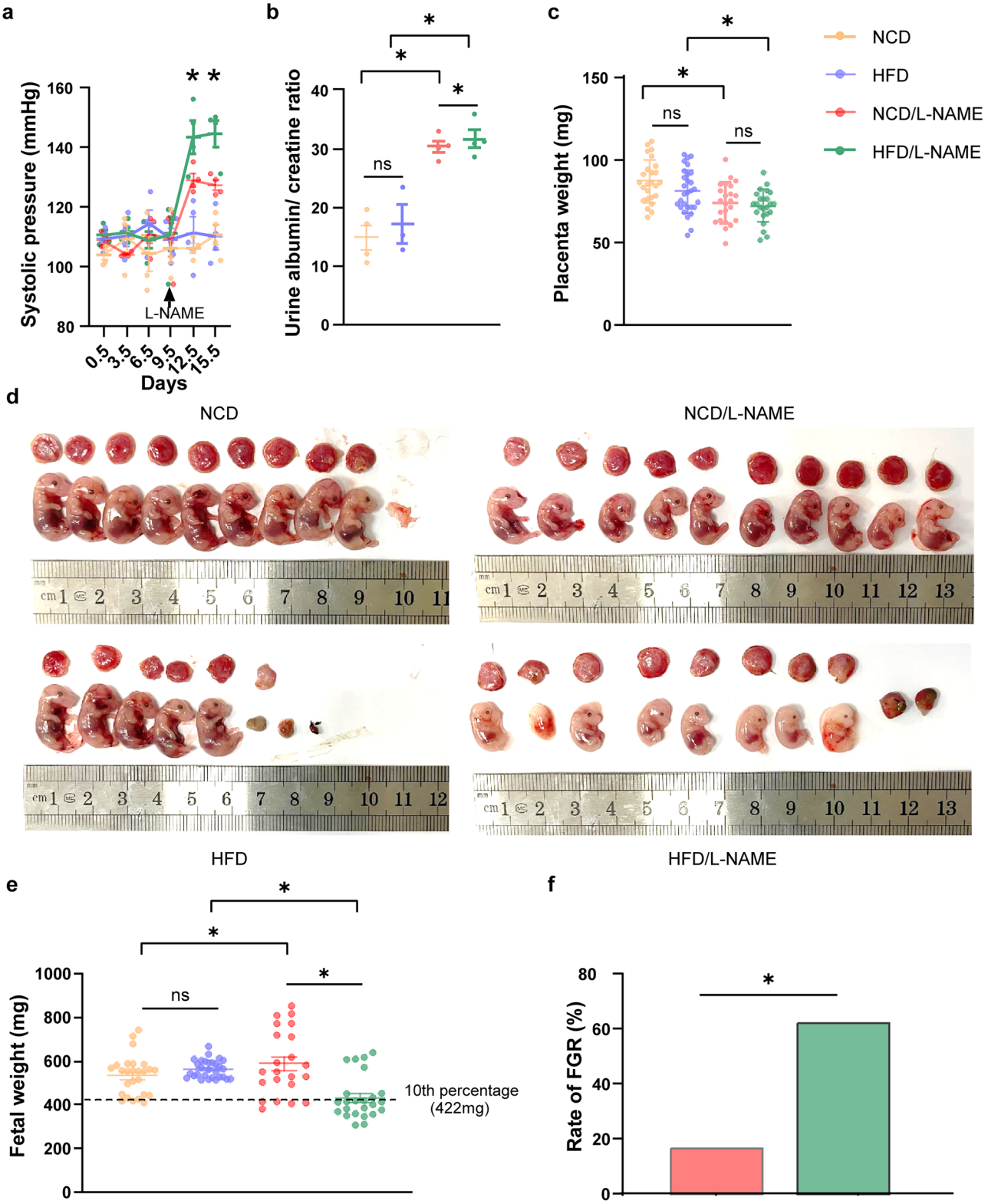

Fig. 1 | High-fat diet aggravated pre-eclampsia-like symptoms in mice. a Systolic blood pressure of control, L-NAME, HFD, and HFD/L-NAME mice at E3.5, E6.5, E9.5, E12.5, and E15.5. **b** 24 h urinary albumin/creatine ratio in each group at E16.5. **c** Placental weight in each group at E18.5. **d** Representative images of the fetus in each group at E18.5. **e** Fetal weight in each group at E18.5. **f** Rate of FGR in L-NAME treated NCD/HFD groups (statistical analysis by Chi-square test). The data are shown as mean ± SEM; $^{*}P < 0.05$.

production of proinflammatory cytokines IL-1β and IL-18 was decreased in supernatant from Swan.71^{C3}. Conversely, they were increased in that of Swan.71$^{\Delta C3}$ (Fig. 5a–c). However, no changes were observed for IFN-γ, GM-CSF (Granulocyte–macrophage colony-stimulating factor), IL-10, IL-17, and MCP-1 production (Fig. 5d–h). These results indicate that cell-autonomous C3 regulated trophoblast-mediated inflammation, especially for some specific cytokine production.

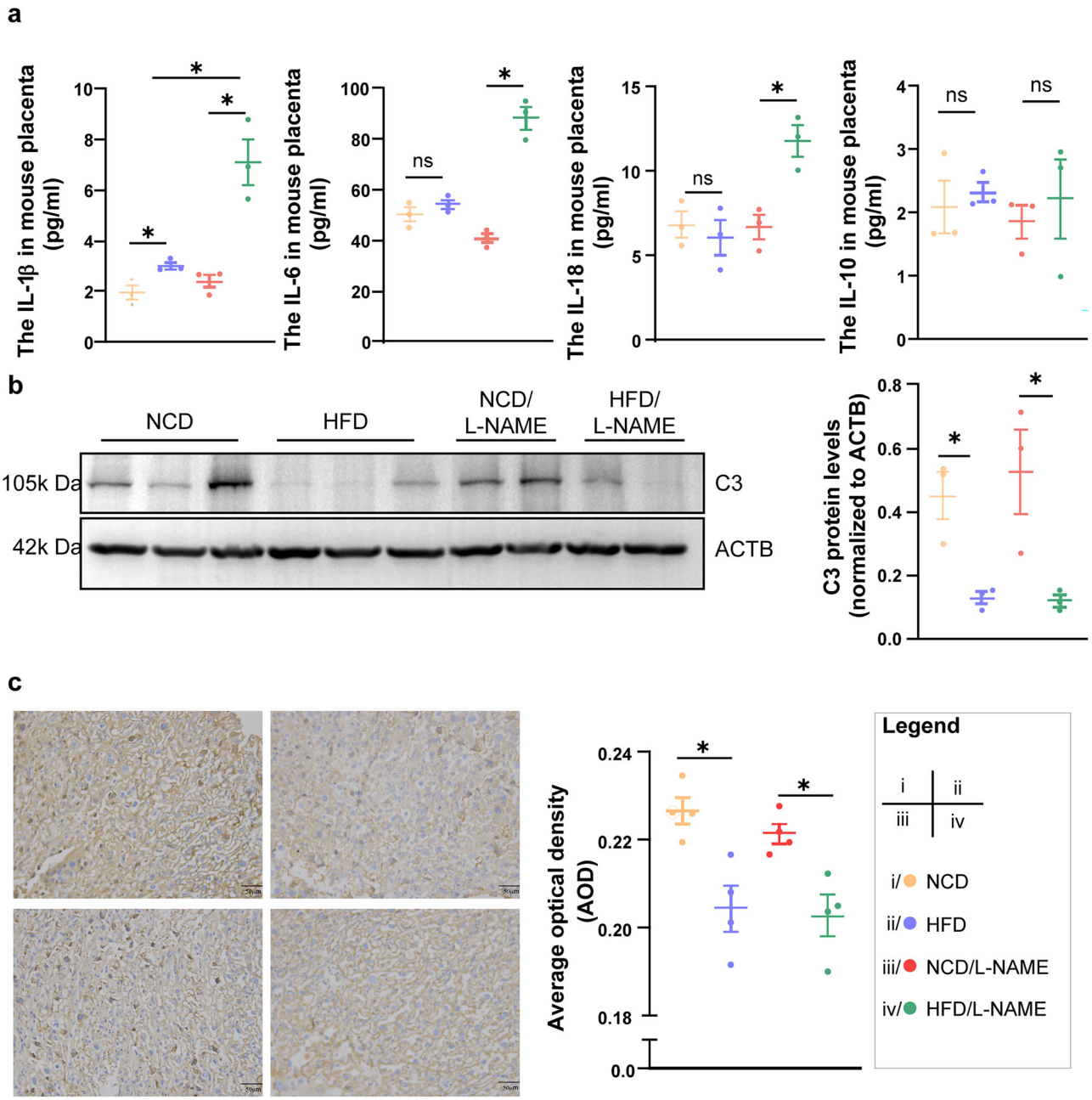

Fig. 2 | Complement C3 levels in high-fat diet-fed mice placentas. a Inflammatory cytokines: IL-1β, IL-6, TNF-α and IL-10 in NCD, L-NAME, HFD and HFD/L-NAME mice at E18.5.**b** Western blot results and statistical analysis for C3 levels in mice placentas. **c** Immunohistochemistry staining showed the C3 protein levels in placentas of NCD, L-NAME, HFD, and HFD/L-NAME mice at E18.5. The data are shown as mean ± SEM; * $P < 0.05$.

Downregulation of C3 promoted inflammasome activation in trophoblasts

As signature cytokines for inflammasome activation, the significant changes of IL-1β and IL-18 in supernatant from Swan.71^{C3} and Swan.71$^{\Delta C3}$ prompted us to investigate whether C3 regulates inflammasome signaling. NLRP3 inflammasome activation is the most-studied pathway, so we first sought to detect the key molecules in the NLRP3 inflammation activation cascade, and found that NLRP3, cleaved caspase-1 were considerably increased in Swan.71$^{\Delta C3}$ cells, indicating that C3 knockdown promoted NLRP3 inflammasome activation in trophoblasts. As inflammasome activation also led to pyroptosis, so we then detected the gasdermin D (GSDMD) cleft, and found that reduced C3 expression significantly promoted GSDMD cleavage, one most critical step for pyroptosis (Fig. 6). These results suggested that C3 regulates inflammation through working on NLRP3 inflammasome activation in trophoblasts.

NLRP3 inflammasome was activated in HFD placentas

As mentioned above, decreased C3 promoted inflammasome activation and pyroptosis in trophoblast, which potentially affects multiple biological behaviors and renders critical effects during PE pathogenesis. Then we further detected the inflammasome activation in HFD/L-NAME mice placentas to verify the role of C3 on inflammasome and inflammation in vivo. Immunoblotting results showed that NLRP3, caspase-1, cleaved caspase-1, GSDMD, and cleaved GSDMD expression were notably elevated in HFD/L-NAME placentas compared with NCD/L-NAME mice (Fig. 7). In addition, the cleaved GSDMD level was also increased in HFD placentas without L-NAME treatment, suggesting the critical effect of HFD on pyroptosis. Totally, these results support the idea that HFD regulates trophoblast-autonomous C3 expression in trophoblast, activates the inflammasome cascade, modulating trophoblast cellular behaviors, which contribute to PE development.

Table 1 | Clinical characteristics of patients with PE

Characteristics	Control ($n = 4$)	Mild PE ($n = 4$)	Severe PE ($n = 4$)
Maternal age (years)	29 ± 3.4	30 ± 2.5	32.8 ± 2.1
Gestational age (weeks)	39 (38–40)	38 (38–39)	36 (32–39)
Systolic blood pressure (mmHg)	112.5 ± 12.4	143 ± 5.9	153 ± 8.2
Diastolic blood pressure (mmHg)	72 ± 4.8	91.3 ± 3.3	98.3 ± 3.8
Proteinuria (mg/24 h)	<300	527.5 ± 214.1	612.5 ± 327.9
Birthweight (g)	2992.5 ± 455.3	2880 ± 331.9	2602.5 ± 262.1
pre-pregnancy BMI	18.2 ± 0.16	22.7 ± 1.41	22.9 ± 2.19
Lipid profiles in first trimester			
Triglyceride (mmol/L)	1.05 ± 0.26	1.77 ± 0.55	1.90 ± 1.00
Total cholesterol (mmol/L)	3.94 ± 0.34	4.30 ± 0.58	4.34 ± 0.65
Low-density lipoprotein cholesterol (mmol/L)	1.73 ± 0.36	1.99 ± 0.44	2.43 ± 0.63
High-density lipoprotein cholesterol (mmol/L)	1.93 ± 0.12	1.88 ± 0.42	1.86 ± 0.34
Placental Cytokine levels			
Interleukin-1β (pg/ml)	2.44 ± 1.58	5.41 ± 1.10*	12.85 ± 5.00
Interleukin-6 (pg/ml)	8.56 ± 3.45	18.02 ± 9.93	26.78 ± 2.57*
Interleukin-18 (pg/ml)	0.88 ± 0.11	1.43 ± 0.30*	2.42 ± 1.94*
Interleukin-10 (pg/ml)	0.07 ± 0.03	0.07 ± 0.03	0.11 ± 0.04

Data are expressed as mean ± SD or median (range).
*Indicated a significant difference compared to the control group ($P < 0.05$).

Discussion

Taking advantage of PE placental tissue samples and L-NAME-induced PE-like mice model, the present study found that cell-autonomous complement C3 in trophoblasts was considerably downregulated in both severe PE patients and HFD/L-NAME mice placentas. Hyperlipidemia/HFD feeding dampens C3 expression in trophoblasts, leading to decreased cellular proliferation, migration, and invasion, which contribute to PE development. Meanwhile, cell-autonomous C3 also regulates anti-angiogenic cytokines secretion in trophoblasts. More importantly, these cellular disorders were potentially mediated by C3 knockdown-induced NLRP3 inflammasome activation, leading to pro-inflammatory cytokine and mediator production. Our study purports another mechanism that cell-autonomous complement C3 in trophoblasts regulates inflammation in HFD-induced PE pathogenesis.

Although it has been assumed that, to some extent, HFD has been shown to contribute to PE[23], previous studies are not consistent. For example, Ge et al. fed 8-week-old rat with HFD during the whole pregnancy and successfully induced PE like symptoms[24], while another study only reported some altered gene expression related to angiogenesis and inflammation in C57BL/6 mice after fed with HFD for 16 weeks, without any differences on the rate of hypertensive disorders of pregnancy from NCD fed mice[25]. This could be due to the mouse strains, the recipe of the chow diet, and the keeping environments. To better understand the effect of HFD on PE, in this study, we established a double-strike mouse model by feeding the mice with HFD combined with L-NAME exposure during pregnancy, which displayed more stable results[26]. Indeed, we observed that HFD exacerbated hypertension and proteinuria in PE mice, hindered placental and fetal development (Fig. 2), while HFD alone could not cause PE in normal pregnant mice. We assumed that the alteration of C3 induced by HFD only was not strong enough to activate the NLRP3 pathway, supporting the assumption that HFD acts as a risk factor for PE and may affect the severity and development of the disease.

Studies have found that obese women showed higher circulating fatty acid levels, and fat deposited in the placenta induced lipotoxicity for trophoblasts and endothelial cells, influencing placental and endothelial functions[27]. Trophoblasts play an important role in implantation and placentation[28,29]. In normal pregnancy, EVTs migrate and invade into the decidua through the uterine interstitium to remodel the spiral artery, which is essential for the establishment of maternal-fetal blood flow. Various studies suggested that insufficient invasion and migration of trophoblasts cause PE[18]. Also, trophoblasts could release anti-angiogenetic factors, including sFlt-1 and sEng, in maternal circulation, which are responsible for the systemic vascular disorder. Thus, we focused on the functional alterations in trophoblasts in the following studies.

Recently, more studies reported that obesity leads to systemic low-grade inflammation, which is essential for PE initiation and development[30]. The complement system, the most-studied innate immunity protein family, plays essential roles in stimulating and regulating inflammatory responses. The activation of complement C3 and C5 has been shown to inhibit regulatory T cells and activate inflammatory T cells, disturbing normal placentation[31]. More recently, intracellular C3 and C5 have been reported to be involved in the inflammatory response by stimulating the generation of IL-1β, while their effect in pregnancy has not been elucidated[32]. In our study, we observed that the C3 expression in trophoblasts was significantly downregulated in HFD-fed mice, providing a hint that HFD may regulate PE development through downregulating C3 expression. We observed that C3 regulated the secretion of anti-angiogenetic sFlt-1 and sEng in trophoblasts, which competitively combine with angiogenetic factors, such as VEGF, placental growth factor, and TGF-β, thus inhibiting angiogenesis and vasodilation, which is a major mechanism in the development of multisystem dysfunction. In addition, we found that C3 promoted trophoblast proliferation and inhibited cell apoptosis, similar to the effect of C3 in airway epithelial cells and myocardial cells[33,34]. In pancreatic cancer cells, intracellular C3 deficiency reduced trophoblast migration and invasion ability through Akt/Smad pathway, and thus inhibited cancer metastasis[35]. In the current study, we noted that C3 knockdown inhibited trophoblast migration and invasion, which led to unsuccessful early placentation and induced severe PE[18]. While overexpression of C3 did not affect cell behaviors, as C3 expression in Swan.71^{C3} cells may not be strong enough to affect downstream pathways. However, the definite pathological role of C3 derived from trophoblasts for PE pathogenesis needs more research, and mice model established based on C3 deficiency specific in trophoblasts would be helpful to clarify this question.

In recent years, the intracellular complement system has been reported to be involved in inflammasome activation. For example, intracellular C5 activation and stimulation of C5aR1 (C5a receptor 1) is essential for inflammasome assembly in Th1 cells[14], and sphingolipid metabolism cleaved intracellular C3 into C3b-α'$_2$ fragments, which could activate NLRP3 through PPIL1 (Peptidylprolyl Isomerase Like 1) in cancer cells[36]. However, in our study, we could not discern whether C3 works intracellularly or by an autocrine style in trophoblasts based on our current results, so we described it as "cell-autonomous C3" in our work to distinguish it from the classic circulating complements. As C3 could be cleaved into C3a, C3b, which is furtherly cleaved into iC3b and other fragments, so to identify the working form of C3 in trophoblasts, we detected C3 using Western Blotting with C3, C3b, and iC3b standard proteins as controls. Although we could not define the working form in placenta tissues, it is pretty clear that it is C3, instead of C3b or iC3b, works to activate inflammasome and other cellular behavior in Swan.71 cells (Figs. 4–6), suggesting that it was C3 who played an important role in regulating placental function. In our study, we found that C3 knockdown in trophoblasts leads to NLRP3 inflammasome activation, but the mechanism remains unknown. Inflammasome activation stimulated inflammatory cytokines secretion and trophoblast pyroptosis, disturbing their normal functions, including invasion and migration[37,38]. Our study witnessed a correlation between the inflammasome and PE pathogenesis, proposing a potential mechanism through which HFD impacts placental functions. It is true that NLRP3 and its

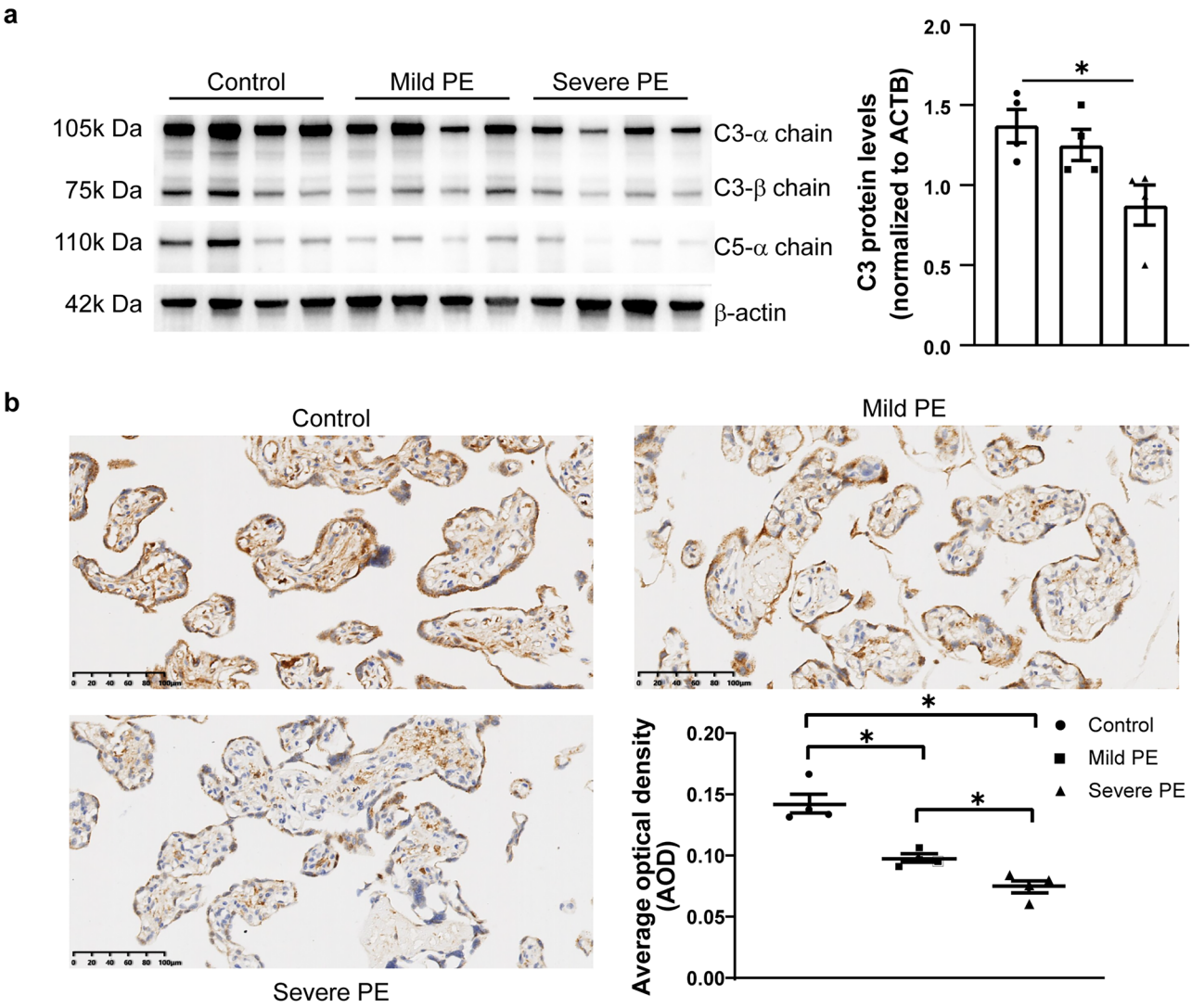

Fig. 3 | Complement C3 levels in pre-eclampsia placentas. a Western blot and **b** immunohistochemistry staining showing the C3 protein levels in placentas of normal pregnancy, mild preeclampsia, and severe preeclampsia.

effector cleaved GSDMD and cleaved caspase-1 were notably reduced in HFD/L-NAME mice placentas, while only cleaved GSDMD was altered in the HFD group, highlighting the aggravating effect of HFD in L-NAME-induced PE mice. Some studies have reported that NLRP3 was activated by HFD in renal injury, obesity, atherosclerosis, and several related diseases[39–41]. Here, our study proposed that HFD triggered NLRP3 via the inhibition of C3, proposing an additional pathway for PE pathogenesis. However, the mechanism underlying how C3 regulated NLRP3 pathway need more studies.

In conclusion, here we present evidence that cell-autonomous complement C3 regulated NLRP3 inflammasome activation upon HFD exposure, affecting the cellular behaviors of trophoblasts, especially in cell viability and motility, which aggravate PE-like symptoms, including maternal hypertension, proteinuria, and FGR. This study proposes a potential candidate target for the prevention and treatment of PE.

Methods

Establishment of animal model

This study was performed on SPF (specific pathogen-free) 6-week-old C57BL/6 female mice, obtained from the Shanghai Model Organisms Center and raised under SPF conditions. All procedures were in compliance with animal protocols approved by the Institutional Animal Care and Use Committee (2022-0015). We have complied with all relevant ethical regulations for animal use. Mice were randomized to the NCD group (normal-chew diet, 10% kcal fat + 20% kcal protein + 70% kcal carbohydrates) and the HFD group (high-fat diet, 60% kcal fat + 20% kcal protein + 20% kcal carbohydrates) and fed for 8 weeks before mating with male mice at a 1:2 ratio. The day when a vaginal plug was observed is defined as day 0.5 of pregnancy. From day 9.5 on gestation (E9.5), water containing L-NAME (1 mg/ml) was fed to NCD and HFD-fed mice to establish PE model; the control group was given normal drinking water. Therefore, pregnant mice were divided into four groups: NCD group; HFD group; NCD/L-NAME group; HFD/L-NAME group. There are at least three mice in each group. HFD was given to mice continuously after mating. Mice were weighed in the 6th week and at E18.5 during pregnancy.

Mice's systolic blood pressure was measured at E3.5, E6.5, E9.5, E12.5, and E15.5 to evaluate the effect of high-fat diet by a non-invasive tail-cuff system (Coda Non-Invasive Blood Pressure System, Kent Scientific Corporation).

Mice's 24 h urine was collected at E16.5. Maternal blood was acquired from angular vein with capillary tube at E18.5. Then, pregnant mice were sacrificed, placenta and fetus were obtained and weighed. All the samples were collected for further analysis.

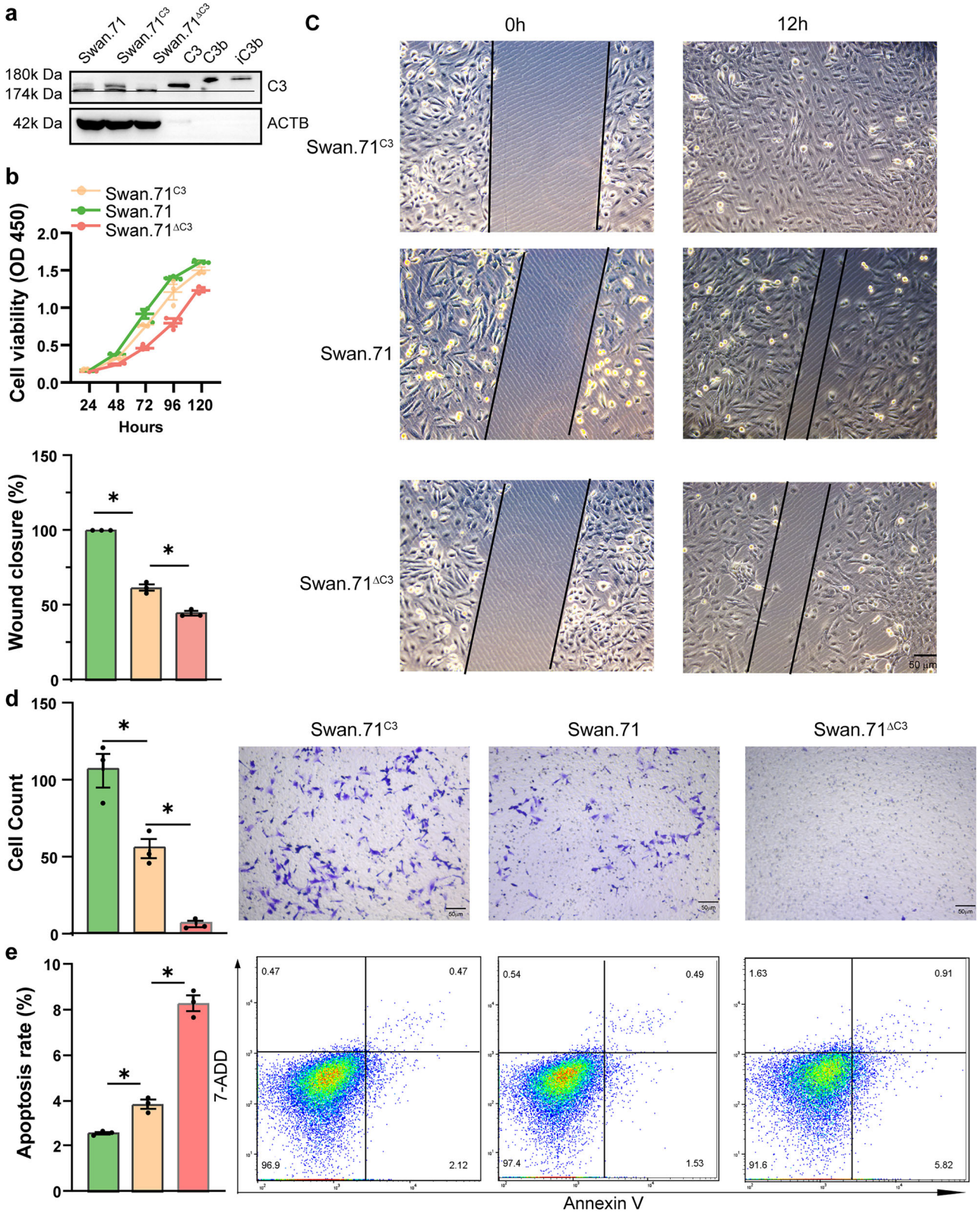

Fig. 4 | The effect of complement C3 on Swan.71 cell function. a Protein expression in C3 overexpression (Swan.71^{C3}), vector control Swan.71 cells and C3 knockdown (Swan.71$^{\Delta C3}$) with C3, C3b and iC3b protein control. **b** Cell viability in Swan.71^{C3}, Swan.71 cells and Swan.71$^{\Delta C3}$ was measured by CCK8. **c** Cell migration detected by wound healing assay in each group. **d** Cell invasion measured by Tanswell assay in each group. **e** Cell apoptosis measured by flow cytometry after staining with Annexin V and 7-ADD. The data are shown as mean ± SEM; * $P < 0.05$; Scale bar: 50 μm.

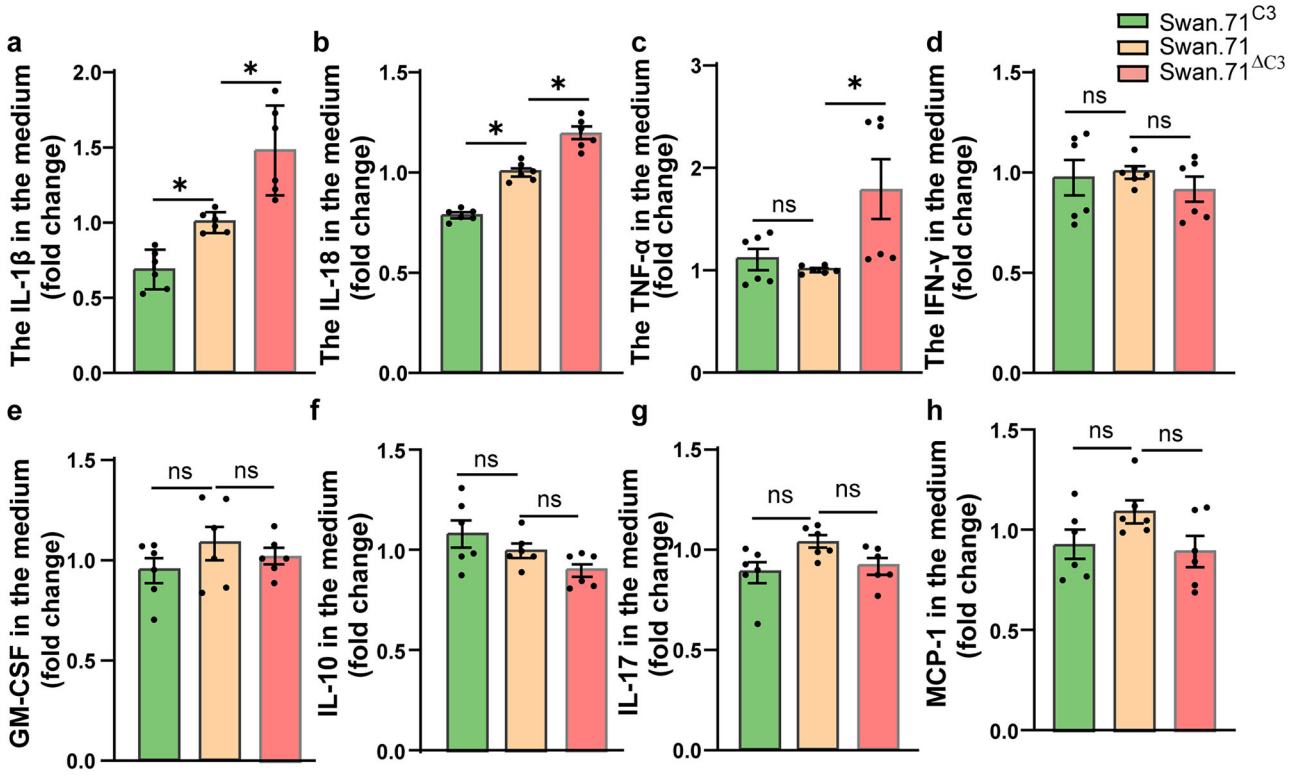

Fig. 5 | Cell-autonomous C3 regulated Swan.71 cell inflammatory cytokines secretion. Inflammatory cytokines (**a**) IL-1β, (**b**) IL-18, (**c**) TNF-α, (**d**) IFN-γ, (**e**) GM-CSF, (**f**) IL-10, (**g**) IL-17 and (**h**) MCP-1 levels in the medium of C3 overexpression (Swan.71^{C3}), C3 knockdown (Swan.71$^{\Delta C3}$) and vector control Swan.71 cells were detected by ELISA. The data are shown as mean ± SEM; *$P < 0.05$.

Human placental tissue collection

Placental tissues from normal pregnant women, mild and severe PE patients aged between 27 and 40 years were collected. All of the involved patients had delivered at International Peace Maternity and Child Health Hospital (IPMCHH) between August 2021 and March 2022. This study was approved by the ethics committee of IPMCHH (GKLW-2017-01). All ethical regulations relevant to human research participants were followed. PE was defined as systolic pressure ≥140 mmHg or diastolic pressure ≥90 mmHg on two or more occasions after gestational week 20, accompanied by proteinuria, and severe PE was diagnosed when PE patients manifested severe hypertension (systolic pressure ≥160 mmHg or diastolic pressure ≥110 mmHg) or symptoms of significant end-organ dysfunction. Patients with gestational diabetes, chronic hypertension, renal disease, intrapartum infection, or other gestational complications were excluded from the study.

The placentas were collected immediately following delivery, and tissues were retrieved from the central portion of the placenta, near the maternal side. After being washed with sterilized phosphate-buffered saline, the tissues were stored at −80 °C for further experiments.

Mice urinary albumin/creatine ratio

Urine albumin levels were detected by ELISA (Enzyme-linked immunosorbent assays, Abcam, UK) and creatine levels were detected in the Laboratory Animal Science Department of Fudan University according to the manufacturer's instructions.

Swan.71 cell culture

Swan.71 is a cell line of human first-trimester trophoblast. The cells were purchased from ATCC cell bank. Swan.71 cells were cultured in DMEM/F12 medium (Gibco, USA) with 10% fetal bovine serum at 37 °C and 5% CO_2.

Lentivirus infection and stable cell line establishment

The overexpression lentivirus was generated by cloning the coding region sequence of C3 into the *Bam*HI/*Age*I sites of GV492 vector (Genechem, China). Three short hairpin RNAs (shRNAs) targeting human C3 gene were inserted into the GV493 vector (Sequence in Supplementary Table1). The lentiviruses were infected in Swan.71 cell line to generate stable infection of cell line following the manufacturer's instructions. 1×10^5 Swan.71 cells in 2 ml medium were infected with 1×10^8 TU/ml lentiviruses. After 48 h, 1 mg/ml, 2 mg/ml, 5 mg/ml, and 10 mg/ml puromycin were added successively for selection. The efficiency of infection was detected by observation of GFP under a fluoroscope.

Cell viability and apoptosis

CCK8 assays (Absin, China) were employed to detect cell viability. 2×10^4 cells were inoculated into 96-well plates and cultured for 5 days. The viability Swan.71 cells of stable infection were detected every 24 h by adding 10% CCK8 assays and measuring the absorbance at 450 nm after 1 h incubation.

Cell apoptosis was detected by Annexin V-PE/7-ADD assays (BD, USA). The apoptotic cells were analyzed by flow cytometry (BD Biosciences, USA). The total apoptotic cells, including early apoptosis cells (Annexin V-PE$^+$ 7-ADD$^-$) and late apoptotic cells (Annexin V-PE$^+$ 7-ADD$^+$).

Cell migration and invasion

Cell wound healing assays were applied to examine trophoblast cell migration. Swan.71 cells at a density of 90% confluence in 6-well plates were scratched with a 200 ml tip. The wound closure rate was calculated as the percentage of wound area at 24 h to 0 h with Image J (National Institutes of Health).

Cell invasion capacity[42] was detected by Transwell assay. The Swan.71 cells resuspended in DMEM/F12 medium were inoculated into Transwell chambers coated with Matrigel. While medium with serum was added in the lower chambers. After 48 h of culture, cells in the upper chambers were completely removed. The remaining cells in the lower chambers were stained and counted.

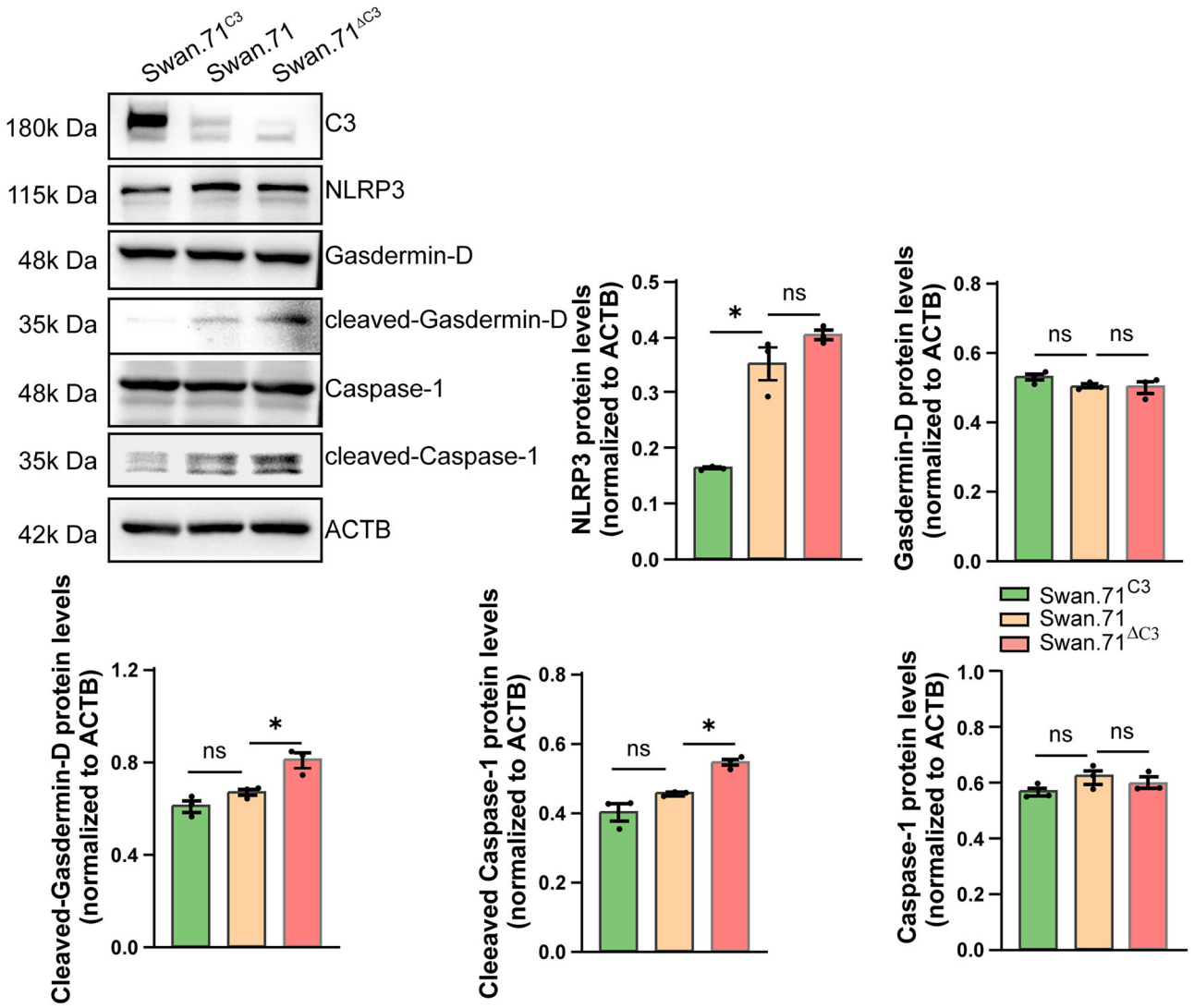

Fig. 6 | C3 knockdown in Swan.71 contributed to NLRP3 inflammasome activation. NLRP3 inflammasome-related protein levels, including NLRP3, GSDMD, cleaved GSDMD, caspase-1, and cleaved caspase-1, were detected by Western blot in C3 overexpression (Swan.71^{C3}), C3 knockdown (Swan.71$^{\Delta C3}$), and vector control Swan.71 cells. The data are shown as mean ± SEM; $^{*}P < 0.05$.

Western blotting

The cell or placenta proteins were extracted using RIPA Buffer (Thermo Fisher Scientific, USA) containing protease inhibitor and phosphatase inhibitor. Proteins were separated by SDS (sodium dodecyl sulfate)-PAGE and then transferred to polyvinylidene fluoride (PVDF) membranes. The PVDF membranes were incubated with various primary antibodies anti-C3/C3a (#ab200999, dilution ratio: 1:2000), and anti-C5/C5a antibody (#ab202039, dilution ratio: 1:1000) from Abcam, UK; anti-NLRP3 (#15101, dilution ratio: 1:1000), anti-Caspase1 (#3866, dilution ratio: 1:1000), anti-cleaved Caspase1 (#4199, dilution ratio: 1:1000), anti-GSDMD (#97558, dilution ratio: 1:1000) and anti-cleaved GSDMD (#4199, dilution ratio: 1:1000) antibody from Cell Signaling Technology, USA) after blocked. After incubation with secondary antibody (#7074, Cell Signaling Technology, USA), immunoreactive bands were visualized with enhanced chemiluminescence.

Cell culture supernatant analysis

The culture supernatant of Swan.71 cell was collected and detected for cytokines, including IL-1β, IL-18, TNF-α, IFN-γ, GM-CSF (Granulocyte-macrophage colony stimulating factor), IL-10, IL-17, and MCP-1 by ELISA kit following the manufacturer's instructions (R&D, USA).

Placental cytokines detection

Human and mice placentas were collected and cytokine levels were analyzed by the Luminex-based multiplex assay (LXLBH10-X, UNIV, China).

IHC staining

The placenta IHC staining was performed with an IHC kit (Absin, China) following the manufacturer's instructions. Paraffin-embedded sections were dewaxed, dehydrated, and antigens retrieved. Then, the slides were blocked and incubated with anti-C3/C3a (#ab20999, dilution ratio: 1:2000, Abcam, USA) and anti-C5/C5a antibodies ((#ab281923, dilution ratio: 1:500, Abcam, USA). They were further incubated with secondary antibodies and stained using DAB and counterstained with hematoxylin. The slides were scanned by HAMAMASTU (Wellbio Technology, China). The staining intensity was evaluated by ImageJ.

Immunofluorescence

The human placental tissue was frozen overnight and embedded with optimal cutting temperature before being cut into sections. The frozen sections were blocked, incubated with primary (anti-C3/C3a, #ab11871, dilution rate: 1:200 and anti-CK7 #ab181598, dilution rate: 1:100) and secondary antibodies (Alexa Flour 488, #A28175, Thermo Fisher Scientific and Alexa Flour 546, #A11035). DAPI (Thermo Fisher Scientific, #62248)

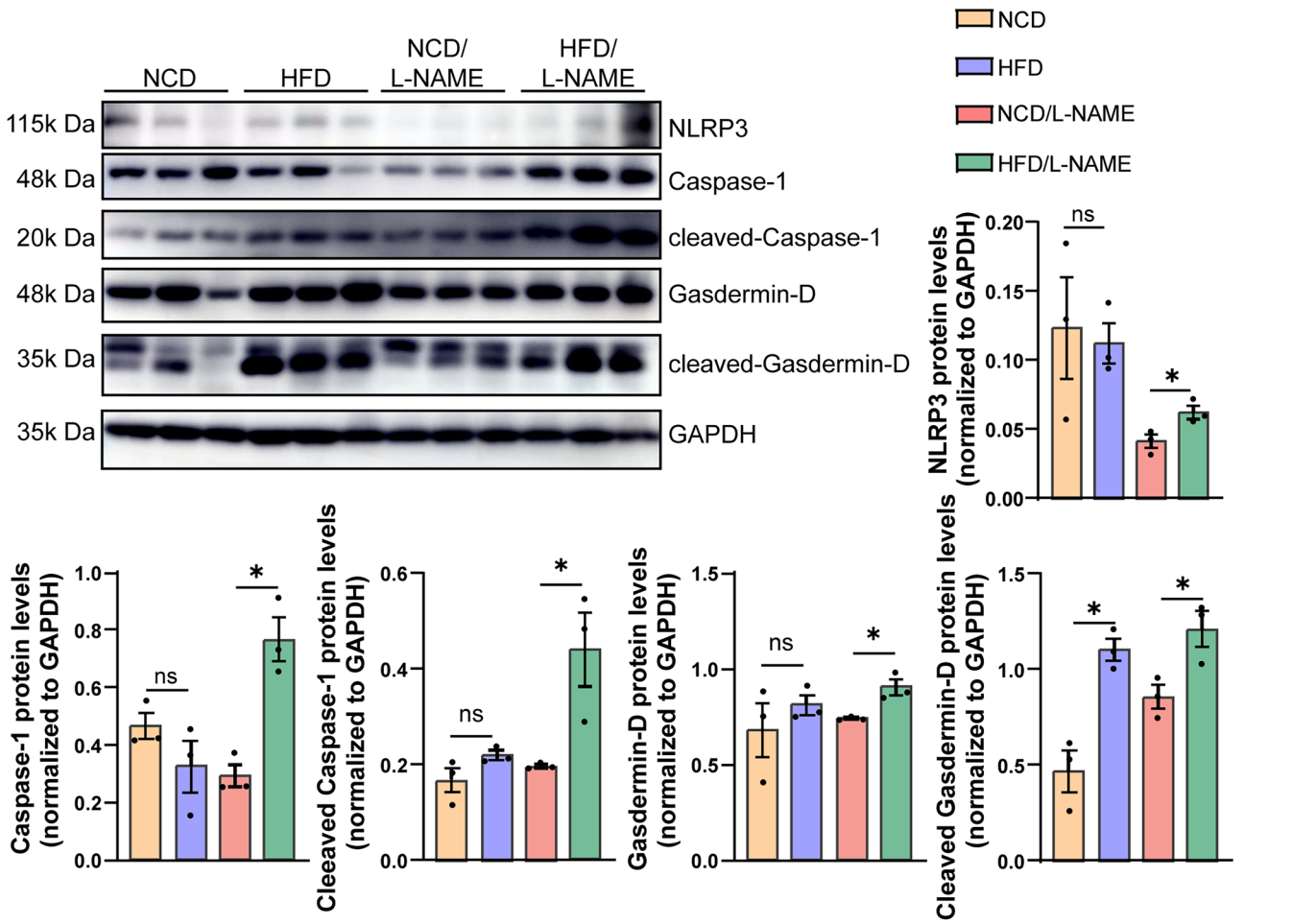

Fig. 7 | High-fat diet induced NLRP3 inflammasome activation in mice placentas. NLRP3 inflammasome-related protein levels were detected by Western blot in L-NAME, HFD, and HFD/L-NAME placentas at E18.5. The data are shown as mean ± SEM; $^{*}P < 0.05$.

was used to stain nuclear. The slides were speculated by a confocal microscope (Leica, German).

Quantitative reverse-transcription PCR (RT-PCR)

Cell total RNA was extracted with RNAiso (Takara, Japan). Total RNA was reverse-transcribed to cDNA using PrimeScript RT Reagent (Takara). To determine gene expression levels, we performed RT-PCR with SYBR Green Fast qPCR Mix Kit (Takara) using a QuantStudio 7 Flex instrument (ThermoFisher Scientific, USA). The primer sequences were shown in Supplmentary Table 1. We used $2^{-\Delta\Delta Ct}$ method to calculate the relative gene expression levels normalized to ACTB (β-actin).

Statistical and reproducibility

All experiments were repeated at least three times biologically and technically. Statistical analysis was performed by GraphPad Prism 8 (GraphPad Software, USA). One-way ANOVA analysis was conducted to compare the statistical differences between three or more groups, while a two-tailed Student's *t* test was used to compare the differences between two groups. $P < 0.05$ was considered as statistically significant. Data are shown as mean value ± SEM.

Study approval

The clinical samples acquisition of this work has been approved by the Ethics Board of IPMCHH (GKLW 2017-01). Written and informed consent was signed by each patient before delivery. Animal experiments were approved by IACUC at Shanghai Model Organism (2022-0015).

Reporting summary

Further information on research design is available in the Nature Portfolio Reporting Summary linked to this article.

Data availability

The experimental data and the simulation results that support the findings of this study are available in Supplementary data. All the uncropped blot images could be found in Supplementary Fig 5.

Received: 13 August 2024; Accepted: 27 May 2025;
Published online: 06 June 2025

References

1. Chen, Q. et al. Small extracellular vesicles-transported lncRNA TDRKH-AS1 derived from AOPPs-treated trophoblasts initiates endothelial cells pyroptosis through PDIA4/DDIT4 axis in preeclampsia. *J. Transl. Med.***21**, 496 (2023).
2. Magee, L. A., Nicolaides, K. H. & von Dadelszen, P. Preeclampsia. *N. Engl. J. Med.* **386**, 1817–1832 (2022).
3. Burton, G. J., Redman, C. W., Roberts, J. M. & Moffett, A. Pre-eclampsia: pathophysiology and clinical implications. *BMJ* **366**, l2381 (2019).
4. Redman, C. W. G., Staff, A. C. & Roberts, J. M. Syncytiotrophoblast stress in preeclampsia: the convergence point for multiple pathways. *Am. J. Obstet. Gynecol.* **226**, S907–S927 (2022).

5. Venkatesh, S. S. et al. Obesity and risk of female reproductive conditions: a Mendelian randomisation study. *PLoS Med.* **19**, e1003679 (2022).
6. Gupta, S., Agarwal, A. & Sharma, R. K. The role of placental oxidative stress and lipid peroxidation in preeclampsia. *Obstet. Gynecol. Surv.* **60**, 807–816 (2005).
7. Spradley, F. T. Metabolic abnormalities and obesity's impact on the risk for developing preeclampsia. *Am. J. Physiol. Regul. Integr. Comp. Physiol.* **312**, R5–R12 (2017).
8. Vandanmagsar, B. et al. The NLRP3 inflammasome instigates obesity-induced inflammation and insulin resistance. *Nat. Med.* **17**, 179–188 (2011).
9. Challier, J. C. et al. Obesity in pregnancy stimulates macrophage accumulation and inflammation in the placenta. *Placenta* **29**, 274–281 (2008).
10. Banadakoppa, M., Balakrishnan, M. & Yallampalli, C. Common variants of fetal and maternal complement genes in preeclampsia: pregnancy specific complotype. *Sci. Rep.* **10**, 4811 (2020).
11. Lokki, A. I. et al. Analysis of complement C3 gene reveals susceptibility to severe preeclampsia. *Front. Immunol.* **8**, 589 (2017).
12. Onat, A. et al. Cross-sectional study of complement C3 as a coronary risk factor among men and women. *Clin. Sci.***108**, 129–135 (2005).
13. Nilsson, B. et al. C3 and C4 are strongly related to adipose tissue variables and cardiovascular risk factors. *Eur. J. Clin. Investig.* **44**, 587–596 (2014).
14. Arbore, G. et al. T helper 1 immunity requires complement-driven NLRP3 inflammasome activity in $CD4^+$ T cells. *Science* **352**, aad1210 (2016).
15. Liszewski, M. K. et al. Intracellular complement activation sustains T cell homeostasis and mediates effector differentiation. *Immunity* **39**, 1143–1157 (2013).
16. Ding, P. et al. Intracellular complement C5a/C5aR1 stabilizes β-catenin to promote colorectal tumorigenesis. *Cell Rep.* **39**, 110851 (2022).
17. Toledo, M. & Singh, R. Complement C3 and autophagy keep the β cell alive. *Cell Metab.* **29**, 4–6 (2019).
18. Pijnenborg, R., Vercruysse, L. & Hanssens, M. Fetal-maternal conflict, trophoblast invasion, preeclampsia, and the red queen. *Hypertens. Pregnancy* **27**, 183–196 (2008).
19. Zhou, R. et al. Complement C3 enhances LPS-elicited neuroinflammation and neurodegeneration via the Mac1/NOX2 pathway. *Mol. Neurobiol.* **60**, 5167–5183 (2023).
20. Zhang, W. et al. CNTNAP4 partial deficiency exacerbates α-synuclein pathology through astrocyte-microglia C3-C3aR pathway. *Cell Death Dis.* **14**, 285 (2023).
21. Kiss, M. G. et al. Cell-autonomous regulation of complement C3 by factor H limits macrophage efferocytosis and exacerbates atherosclerosis. *Immunity* **56**, 1809–1824.e1810 (2023).
22. Deer, E. et al. The role of immune cells and mediators in preeclampsia. *Nat. Rev. Nephrol.* **19**, 257–270 (2023).
23. Jung, E. et al. The etiology of preeclampsia. *Am. J. Obstet. Gynecol.* **226**, S844–S866 (2022).
24. Ge, J. et al. Why does a high-fat diet induce preeclampsia-like symptoms in pregnant rats. *Neural Regen. Res.* **8**, 1872–1880 (2013).
25. Mahany, E. B. et al. Obesity and high-fat diet induce distinct changes in placental gene expression and pregnancy outcome. *Endocrinology* **159**, 1718–1733 (2018).
26. Sun, M. N., Yang, Z. & Ma, R. Q. Effect of high-fat diet on liver and placenta fatty infiltration in early onset preeclampsia-like mouse model. *Chin. Med. J.***125**, 3532–3538 (2012).
27. Jarvie, E. et al. Lipotoxicity in obese pregnancy and its potential role in adverse pregnancy outcome and obesity in the offspring. *Clin. Sci.***119**, 123–129 (2010).
28. Carter, A. M., Enders, A. C. & Pijnenborg, R. The role of invasive trophoblast in implantation and placentation of primates. Philos. Trans. R. Soc. B **370**, 20140070 (2015).
29. Knöfler, M. et al. Human placenta and trophoblast development: key molecular mechanisms and model systems. *Cell Mol. Life Sci.* **76**, 3479–3496 (2019).
30. Cantin, C., Arenas, G., San Martin, S. & Leiva, A. Effects of lipoproteins on endothelial cells and macrophages function and its possible implications on fetal adverse outcomes associated to maternal hypercholesterolemia during pregnancy. *Placenta* **106**, 79–87 (2021).
31. Regal, J. F., Burwick, R. M. & Fleming, S. D. The complement system and preeclampsia. *Curr. Hypertens. Rep.* **19**, 87 (2017).
32. West, E. E. & Kemper, C. Complosome - the intracellular complement system. *Nat. Rev. Nephrol.* **19**, 426–439 (2023).
33. Kulkarni, H. S. et al. Intracellular C3 protects human airway epithelial cells from stress-associated cell death. *Am. J. Respir. Cell Mol. Biol.* **60**, 144–157 (2019).
34. Torp, M. K. et al. Intracellular complement component 3 attenuated ischemia-reperfusion injury in the isolated buffer-perfused mouse heart and is associated with improved metabolic homeostasis. *Front. Immunol.* **13**, 870811 (2022).
35. Suzuki, R. et al. Intracellular C3 modulates EMT via the Akt/Smad pathway in pancreatic cancer cells. *Anticancer Res.* **42**, 5743–5750 (2022).
36. Janneh, A. H. et al. Crosstalk between pro-survival sphingolipid metabolism and complement signaling induces inflammasome-mediated tumor metastasis. *Cell Rep.* **41**, 111742 (2022).
37. Cheng, S. B. et al. Pyroptosis is a critical inflammatory pathway in the placenta from early onset preeclampsia and in human trophoblasts exposed to hypoxia and endoplasmic reticulum stressors. *Cell Death Dis.* **10**, 927 (2019).
38. Wu, H. Y., Liu, K. & Zhang, J. L. LINC00240/miR-155 axis regulates function of trophoblasts and M2 macrophage polarization via modulating oxidative stress-induced pyroptosis in preeclampsia. *Mol. Med.* **28**, 119 (2022).
39. Jiang, J., Ding, S., Zhang, G. & Dong, Y. Ambient particulate matter exposure plus a high-fat diet exacerbate renal injury by activating the NLRP3 inflammasome and TGF-β1/Smad2 signaling pathway in mice. *Ecotoxicol. Environ. Saf.* **238**, 113571 (2022).
40. Fan, R. et al. Red Raspberry Polyphenols attenuate high-fat diet-driven activation of NLRP3 inflammasome and its paracrine suppression of adipogenesis via histone modifications. *Mol. Nutr. Food Res.* **64**, e1900995 (2020).
41. Zhang, R. et al. Cereal fiber ameliorates high-fat/cholesterol-diet-induced atherosclerosis by modulating the NLRP3 inflammasome pathway in ApoE(–/–) Mice. *J. Agric. Food Chem.* **66**, 4827–4834 (2018).
42. Justus, C. R., Marie, M. A., Sanderlin, E. J. & Yang, L. V. Transwell in vitro cell migration and invasion assays. *Methods Mol. Biol.* **2644**, 349–359 (2023).

Acknowledgments

We thank all the doctors and nurses who helped with the placenta collection for the study. We also thanked the pregnant women who provided the placenta tissues in the current study. This work is supported by National Key Research and Development Program of China (2021YFC2700700, 2022YFC2703500), National Natural Science Foundation of China (82088102, 82171686, 82171812), CAMS Innovation Fund for Medical Sciences (2019-I2M-5-064), Collaborative Innovation Program of Shanghai Municipal Health Commission (2020CXJQ01), Key Discipline Construction Project (2023-2025) of Three-Year Initiative Plan for Strengthening Public Health System Construction in Shanghai (GWVI-11.1-35), Clinical research program of Shanghai Municipal Health Commission (202340222), Natural Science Foundation of Shanghai (20ZR1463100), Clinical Research Plan of Shanghai Shenkang Hospital Development Center (SHDC2023CRD001, SHDC2020CR1008A), China Postdoctoral Science Foundation (2024M762046), Shanghai Clinical Research Center for Gynecological Diseases (22MC1940200), Shanghai Urogenital System Diseases Research

Center (2022ZZ01012) and Shanghai Frontiers Science Research Center of Reproduction and Development.

Author contributions

S.Z., S.C., Y.G., F.Z., and K.S. performed the experiments; S.Z. and S.C. analyzed the data; S.Z. interpreted the results, prepared the figures, and drafted the manuscript; H.H., Y.W., and C.X. edited and revised the manuscript; H.H. conceived and designed the research.

Competing interests

The authors declare no competing interests.

Additional information

Supplementary information The online version contains supplementary material available at https://doi.org/10.1038/s42003-025-08298-z.

Correspondence and requests for materials should be addressed to Congfeng Xu, Yanting Wu or Hefeng Huang.

Peer review information *Communications Biology* thanks the anonymous reviewers for their contribution to the peer review of this work. Primary Handling Editor: Ophelia Bu. A peer review file is available.